

SIMPLE MODELS FOR THE SEISMIC RESPONSE OF RIGID OR FLEXIBLE BLOCKS

S. Diamantopoulos¹, M. Fragiadakis²

¹ Laboratory for Earthquake Engineering
National Technical University of Athens (NTUA)
9 Iroon Polytechniou 15780, Zografou Campus, Athens, Greece
e-mail: s.diam@outlook.com.gr

² Laboratory for Earthquake Engineering
National Technical University of Athens (NTUA)
9 Iroon Polytechniou 15780, Zografou Campus, Athens, Greece
e-mail: mfrag@mail.ntua.gr

Keywords: rocking structures, rigid blocks, flexible blocks, seismic response, FEM modeling, non-linear response history analysis.

Abstract. *The paper examines different approaches for modeling the seismic response of blocks that are either rigid or flexible. Simple models that are based on beam-column elements and can be implemented with common finite element (FE) software are developed. We first study rigid blocks and we compare our findings with results obtained solving directly the block's equation of motion as derived by Housner's theory. We compare different single-degree-of-freedom (SDOF) models which consist of a rigid beam connected to a zero-length, non-linear rotational spring with negative-stiffness, while different options for modelling energy dissipation are considered. The proposed models are compared using simple wavelets and natural ground motion records producing accurate results in all cases. The proposed FE approach allows to also study flexible blocks offering a modeling that is simple and able to provide very accurate solutions using tools that are widely available in existing software, or easy to implement in a FE code.*

1 INTRODUCTION

Free-standing slender blocks can uplift, rock or overturn [1, 2]. Rocking is the partial uplift of a rigid, or a flexible, structure from its base when the center of rotation changes. The solution of the rocking problem should take into account a wide range of non-linear phenomena such as impact, contact, sliding and uplift that occur during a rocking motion. As a result, many studies on the solitary rigid block have been presented for more than a century [3]. Research on the dynamic response of rocking structures is focused on developing methods that answer whether the structure will overturn or it will rock safely, while there are also many studies that propose means for the seismic protection of rocking structures. Several models and approaches for the numerical modeling of blocks have been proposed and are able to assess the rocking response of both rigid and flexible bodies (e.g. [4, 5]). Block flexibility complicates further the dynamic response of these structures, while many researchers, e.g. Psycharis [6], Apostolou et al. [7], and Acikgoz and Dejong [8] have studied their seismic response.

In this paper equivalent Single-Degree-of-Freedom (SDOF) models are proposed for solving the rocking block problem. The models include an elastic column (rigid or deformable) with a cross section similar to that of the block. The SDOF oscillator is connected to the ground with a zero-length, non-linear elastic rotation spring, as originally proposed by Vasiliou et al. [4]. We first consider only rigid blocks and we then extend the concept to the case of flexible systems. Moreover, energy dissipation in rocking bodies takes place instantaneously at every impact. Several finite element (FE) models use continuous viscous damping (e.g. Rayleigh damping) to quantify the energy dissipated by the structure during a ground motion [4]. This approach is not appropriate since energy dissipation is primarily instantaneous and takes place on every impact [9]. We propose instead an event-based damping scheme, which when combined with our simplified FE model it is able to produce accurate response estimates. Our approach correlates the coefficient of restitution with the angular velocity of the block and is validated against Housner's theory.

2 SEISMIC RESPONSE OF UNDAMPED RIGID ROCKING BLOCKS

A homogeneous rigid block with height $2h$ and width $2b$ is considered (Fig. 1). We assume that the coefficient of friction between the block and the rigid base is always big enough to prevent sliding. The block has weight W , mass m and its moment of inertia about the point O is I_o (Fig. 1). Furthermore, θ is the response rotation, $\alpha = \arctan(b/h)$ is the block slenderness and $R = \sqrt{b^2 + h^2}$ is the size parameter of the block. The latter two parameters describe fully a block's geometry, while g denotes the acceleration of gravity.

Taking into account that the body remains at the same position at the instant of impact, the equation of motion of a free-standing block under a horizontal ground acceleration \ddot{u}_g is obtained from the equilibrium between the overturning and the restoring moment. If the restoring moment is $M_{rst} = I_o \ddot{\theta}(t) + mgR \sin[\alpha \operatorname{sgn} \theta(t) - \theta(t)]$, and the overturning moment is given from the expression $M_{ovtn} = -m\ddot{u}_g(t) R \cos[\alpha \operatorname{sgn} \theta(t) - \theta(t)]$, the equation of motion will be [1, 10, 11, 12]:

$$I_o \ddot{\theta}(t) + mgR \sin[\alpha \operatorname{sgn} \theta(t) - \theta(t)] = -m\ddot{u}_g(t) R \cos[\alpha \operatorname{sgn} \theta(t) - \theta(t)] \quad (1)$$

The block will start rocking only when the ground acceleration exceeds a threshold value, i.e. when $\ddot{u}_g \geq (b/h)g = g \tan \alpha$. Moreover, for a rectangular block $I_o = 4/3mR^2$ and if we set $p = \sqrt{(3g)/(4R)}$, where p is the parameter of frequency of the rocking block, the block's

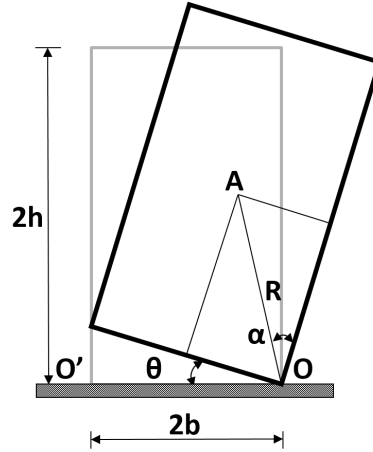


Figure 1: Rocking block geometry.

equation of motion takes the form:

$$\ddot{\theta}(t) = p^2 [-\sin[\alpha \operatorname{sgn} \theta(t) - \theta(t)] - \ddot{u}_g(t)/g \cos[\alpha \operatorname{sgn} \theta(t) - \theta(t)]] \quad (2)$$

Assuming that θ and α are small we can linearize the equation of motion and simplify it:

$$\ddot{\theta}(t) = p^2 [-[\alpha \operatorname{sgn} \theta(t) - \theta(t)] - \ddot{u}_g(t)/g] \quad (3)$$

The above expressions can be solved numerically using standard Ordinary Differential Equation (ODE) solvers. All results produced in this study were obtained with the aid of the ODE23s solver available in Matlab's [13] library.

3 SIMULATION OF ROCKING BLOCKS WITH SIMPLE SDOF MODELS

The need for a simple and robust solution algorithm for rigid block structures led us to the development of simplified single-degree-of-freedom (SDOF) models. These models can be implemented within finite element (FE) codes which are extensively used in engineering practice. Furthermore, this approach allows to easily handle flexible rocking bodies and can be extended to many other applications circumventing the need for specifically tailored analytical solutions. Following the concept originally proposed by Vassiliou et al. [4], we examine four simple SDOF models in order to calculate the motion of rigid rectangular blocks. The extension of this modeling to flexible blocks is also discussed. All models are based on an rigid/flexible SDOF oscillator with moment of inertia and modulus of elasticity identical to those of the block. The oscillator is connected at its base with a zero-length, non-linear rotational spring in order to simulate the restoring moment of the block (Fig. 2).

Figure 3a shows the moment-rotation relationship of the nonlinear spring during the rocking motion of a solitary free-standing rigid block. Moment equal to $M_o = mgb = mgR \sin \alpha$ is required for setting the block from its rest position ($\theta = 0$) to rocking motion. Once the block is set to rocking motion the restoring moment decreases (negative stiffness), reaching zero when the block overturns at $\theta = \alpha$. The moment-rotation relationship is introduced in the models setting the negative stiffness of the rocking block equal to $k_b = mgR \sin(\alpha - \theta)$ according to Eq. 1. This expression can be simplified to $k_b = mgR \sin \alpha (1 - \theta/\alpha)$, thus having a linear relationship for the negative stiffness. The two options are shown in Fig. 3a and b,

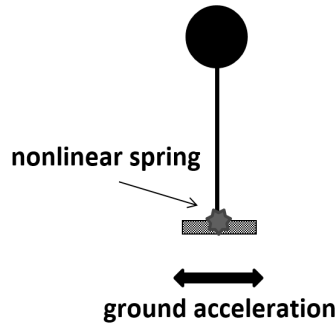


Figure 2: Single-degree-of-freedom (SDOF) rigid block model.

respectively. In both cases, unloading-reloading should follow exactly the same path, thus a pertinent material model should be available. A third option is using a rigid-perfectly plastic moment-rotation relationship with moment capacity equal to $M_o = mgR \sin \alpha$ (Fig. 3c) [4]. In this case the negative stiffness is introduced assuming full geometric non-linearity with second-order analysis.

All three options are possible thanks to the versatility of OpenSees [14] which offers pertinent material models and also can be used in large displacement-small strain problems. Furthermore, typically the first branch of most material models is linear elastic. If such a material model is adopted, a “yield” rotation defining a big initial stiffness value should be adopted. This can be easily achieved setting the “yield” rotation to very small values, e.g. $10^{-5} \div 10^{-12}$. Our parametric analyses have shown that the differences between the first two options of Fig. 3 (cases a, b) are negligible, while the third option (Fig. 3c) produces errors in some cases and depending on the model considered. In the remaining of this work our results have been obtained using the negative stiffness relationship assuming that the negative stiffness is constant, i.e. case b of Fig. 3, unless otherwise specified. The latter option is more easy to implement compared to first case and is also more stable compared to the third option.

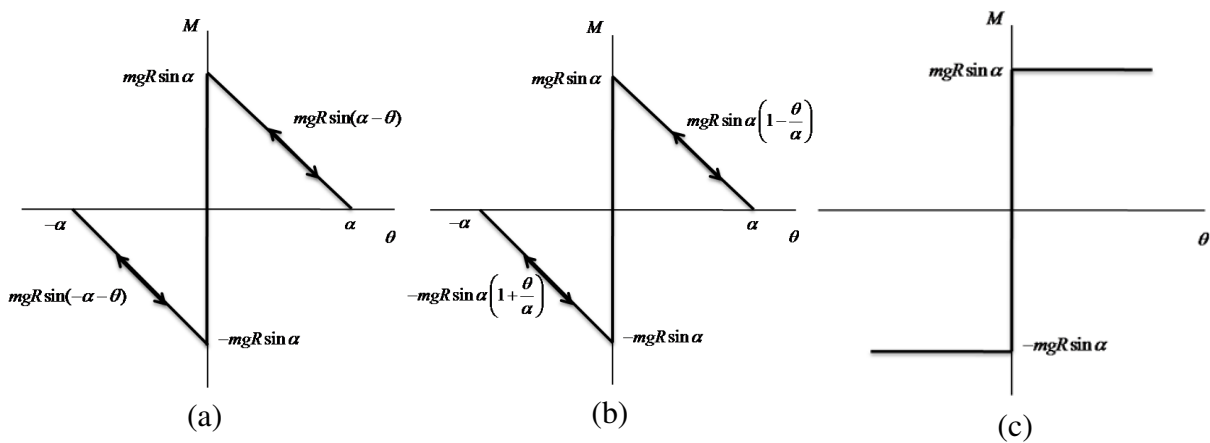


Figure 3: Moment-rotation relationships of the non-linear elastic rotation spring used in the SDOF models.

3.1 Spring Model 1 (SM1)

The first model considered is denoted as Spring Model 1 (SM1) and is shown conceptually in Figure 4. The model assumes that the block's mass is concentrated at its center (point A , Fig. 4). If the moment of inertia about the center A is $I_A = (1/3)mR^2$, its value with respect to point O (or O') will be $I_o = 1/3mR^2 + mR^2 = 4/3mR^2$. The negative stiffness is taken into account through the stiffness of the spring.

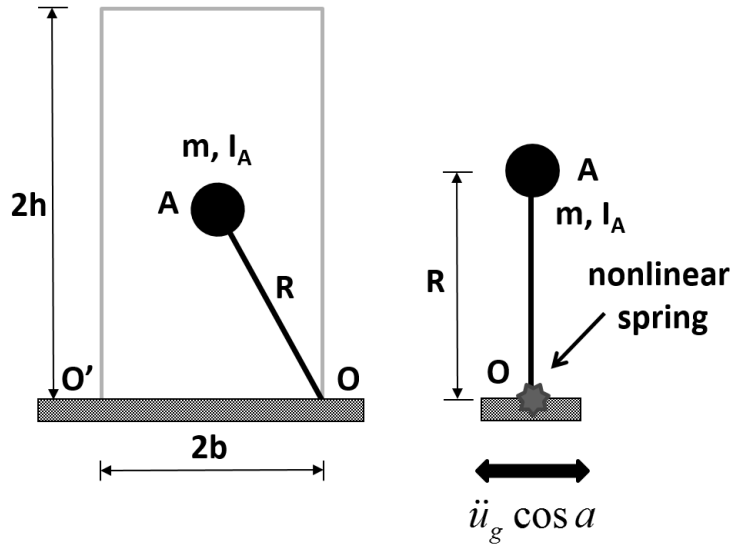


Figure 4: Single degree of freedom Spring Model 1 (SM1).

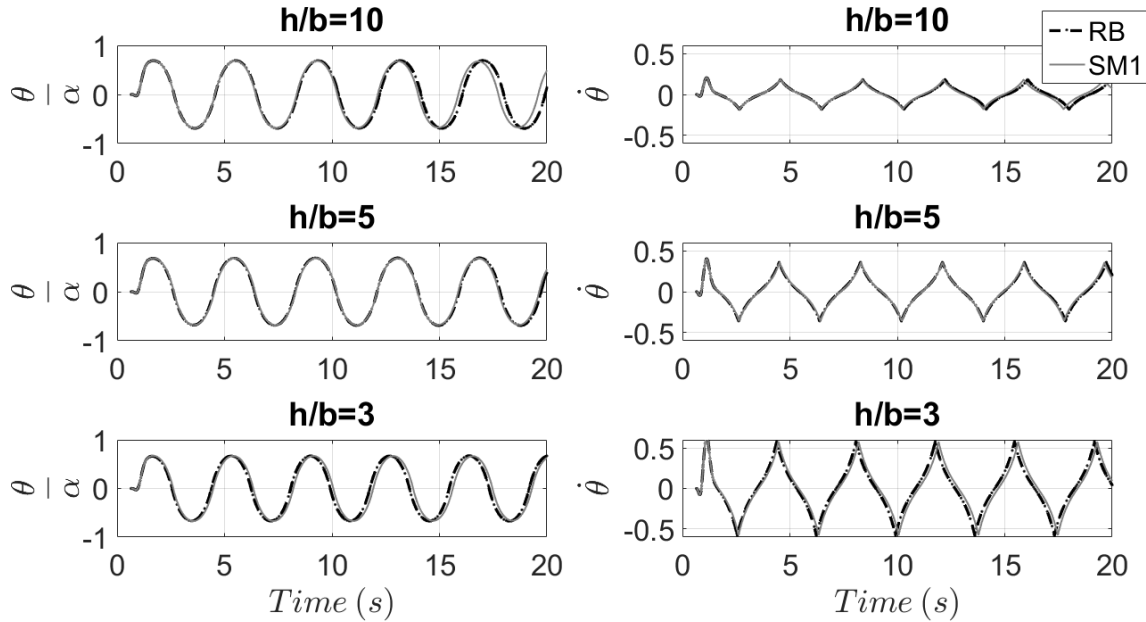


Figure 5: Comparison of rocking rotation and velocity response history between the rocking block (RB) and the SM1 model for a block with $R = 2m$ subjected to a symmetric Ricker pulse excitation with $\alpha_p = 3.6g \tan \alpha$ and $\omega_p = 3\pi \text{ rad/s}$.

For the three different moment-rotation relationships of Fig. 3, the equations of motion of the SM1 model are as follows:

$$I_o \ddot{\theta}(t) + mgR \sin [\alpha \operatorname{sgn} \theta(t) - \theta(t)] = -m(\ddot{u}_g(t) \cos \alpha) R \cos \theta(t) \quad (4)$$

$$I_o \ddot{\theta}(t) + mgR \sin \alpha \operatorname{sgn} \theta(t) [1 - \theta(t) \operatorname{sgn} \theta(t) / \alpha] = -m(\ddot{u}_g(t) \cos \alpha) R \cos \theta(t) \quad (5)$$

$$I_o \ddot{\theta}(t) + mgR [\sin \alpha \operatorname{sgn} \theta(t) - \sin \theta(t)] = -m(\ddot{u}_g(t) \cos \alpha) R \cos \theta(t) \quad (6)$$

Considering the exact matching of the restoring moments between the SM1 with the negative stiffness relationship and the RB, the only difference in the equations of motion arise from the overturning moment terms. The overturning moment of the rocking block (RB) is $M_{ovtn} = -m\ddot{u}_g(t) R \cos [\alpha \operatorname{sgn} \theta(t) - \theta(t)]$ while for the SM1 it is $M'_{ovtn} = -m\ddot{u}_g(t) R \cos \alpha \cos \theta(t)$. Figure 5 compares the rotation θ , which is the response quantity of interest, versus the solution of the block's equation of motion (Eq. 1) with Matlab that will be here referred as “Rocking Block” (RB). The obtained results agree perfectly for slenderness values shown.

3.2 Spring Model 2 (SM2)

The second spring model (SM2) assumes that the mass of the block is concentrated at the pivot point (Fig. 6). This derivation is obtained comparing Eq. 1 with the equation of motion of a SDOF oscillator: $m\ddot{u} + c\dot{u} + ku = -m\ddot{u}_g$. In the case of the block, the d.o.f of interest is the rotation θ as opposed to the displacement u of the SDOF oscillator. In rotational motion the mass is replaced by the moment of inertia $I_o = (4/3)mR^2$. The stiffness is considered through the stiffness of the spring. After manipulating the equation of motion, we find that the ground motion should be applied on the rotational degree-of-freedom multiplied with $3\cos\alpha/4R$.

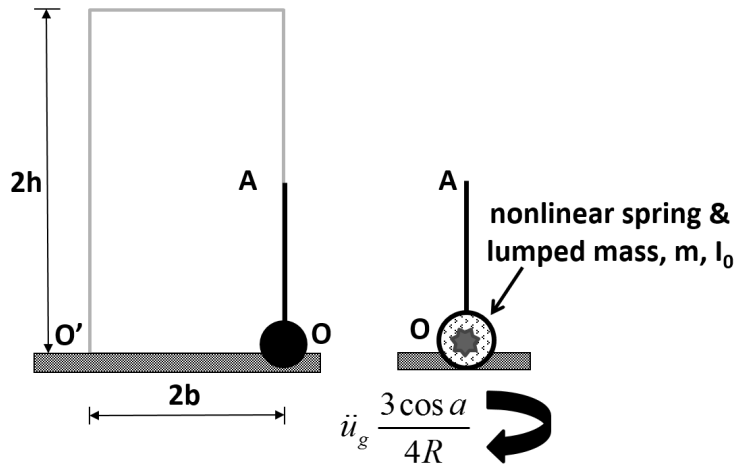


Figure 6: Single degree of freedom Spring Model 2 (SM2).

The equation of motion of the SM2 model, for each of the three moment-rotation relationships of Fig. 3, respectively, will be:

$$I_o \ddot{\theta}(t) + mgR \sin [\alpha \operatorname{sgn} \theta(t) - \theta(t)] = -I_o(\ddot{u}_g(t) 3 \cos \alpha / 4R) \cos \theta(t) \quad (7)$$

$$I_o \ddot{\theta}(t) + mgR \sin \alpha \operatorname{sgn} \theta(t) [1 - \theta(t) \operatorname{sgn} \theta(t) / \alpha] = -I_o(\ddot{u}_g(t) 3 \cos \alpha / 4R) \cos \theta(t) \quad (8)$$

$$I_o \ddot{\theta}(t) + mgR [\sin \alpha \operatorname{sgn} \theta(t) - \cos \alpha \sin \theta(t)] = -I_o(\ddot{u}_g(t) 3 \cos \alpha / 4R) \cos \theta(t) \quad (9)$$

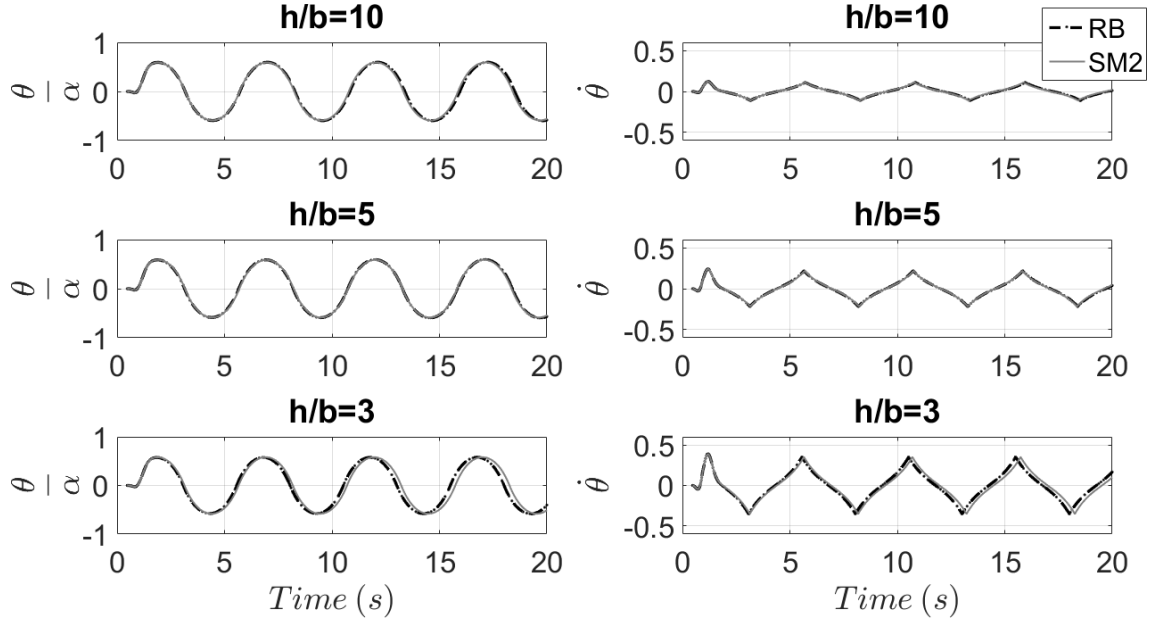


Figure 7: Comparison of rocking rotation and velocity response history between the rocking block (RB) and the SM2 model for a block with $R = 5m$ subjected to a symmetric Ricker pulse excitation with $\alpha_p = 3.6g \tan \alpha$ and $\omega_p = 2\pi \text{ rad/s}$.

If the negative stiffness is that of Fig. 3b, the restoring moments of SM2 and RB are identical. As a result, the only difference in the equations of motion is in the term of the overturning moments. The overturning moment of the rocking block is $M_{ovtn} = -m\ddot{u}_g(t) R \cos[\alpha \text{sgn}\theta(t) - \theta(t)]$ while for the SM2 it is $M'_{ovtn} = -I_o(\ddot{u}_g(t) 3 \cos \alpha / 4R) \cos \theta(t) = -m\ddot{u}_g(t) R \cos \alpha \cos \theta(t)$. Figure 7 compares the response of the rocking block and SM2, when subjected to a symmetric Ricker pulse. Perfect agreement is observed for all slenderness values considered.

3.3 Spring Model 3 (SM3)

Spring Model 3 (SM3) assumes that the mass of the block is concentrated at the center of the block (point A), while the pivot point is its projection on the base (Fig. 8). The moment of inertia with respect to point A is $I_A = 1/3mR^2 + mb^2$, while about O it is $I_o = (1/3)mR^2 + mb^2 + mh^2 = \dots = (4/3)mR^2$, thus equal to the moment of inertia of the block. Since the stiffness is considered through the stiffness of the spring, comparing with the equation of motion of the rocking block (Eq. 1), the only difference is in the overturning moment term since the overturning moment of the rocking block is $M_{ovtn} = -m\ddot{u}_g(t) R \cos[\alpha \text{sgn}\theta(t) - \theta(t)]$ while of the SM3 is $M'_{ovtn} = -m\ddot{u}_g(t) R \cos \alpha \cos \theta(t)$. The corresponding equations of motion that take into account the three moment-rotation relationships of Figure 3 are as follows:

$$I_o\ddot{\theta}(t) + mgR \sin[\alpha \text{sgn}\theta(t) - \theta(t)] = -m\ddot{u}_g(t) (R \cos \alpha) \cos \theta(t) \quad (10)$$

$$I_o\ddot{\theta}(t) + mgR \sin \alpha \text{sgn}\theta(t) [1 - \theta(t) \text{sgn}\theta(t) / \alpha] = -m\ddot{u}_g(t) (R \cos \alpha) \cos \theta(t) \quad (11)$$

$$I_o\ddot{\theta}(t) + mgR[\sin \alpha \text{sgn}\theta(t) - \cos \alpha \sin \theta(t)] = -m\ddot{u}_g(t) (R \cos \alpha) \cos \theta(t) \quad (12)$$

Rotation and velocity response histories for three different slenderness values ($h/b = 2, 5, 10$) and $R = 10m$ under a symmetric Ricker pulse are shown in Figure 9. Excellent agreement with the results of the rocking block theory is observed again.

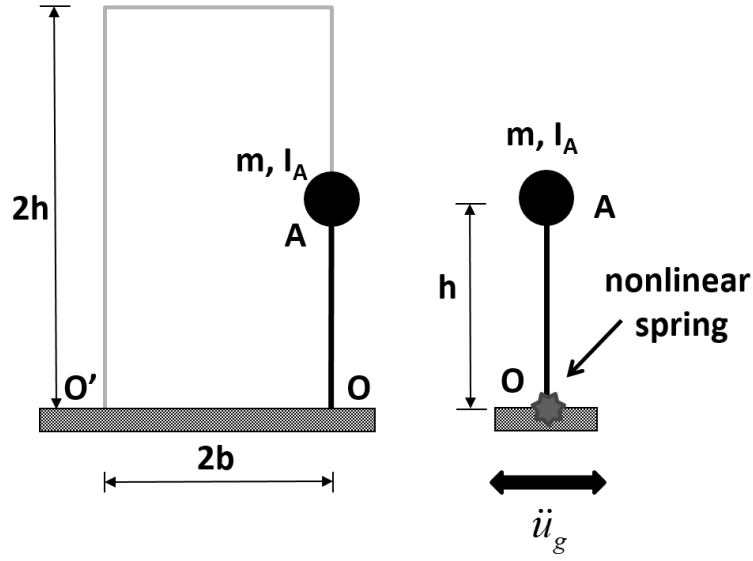
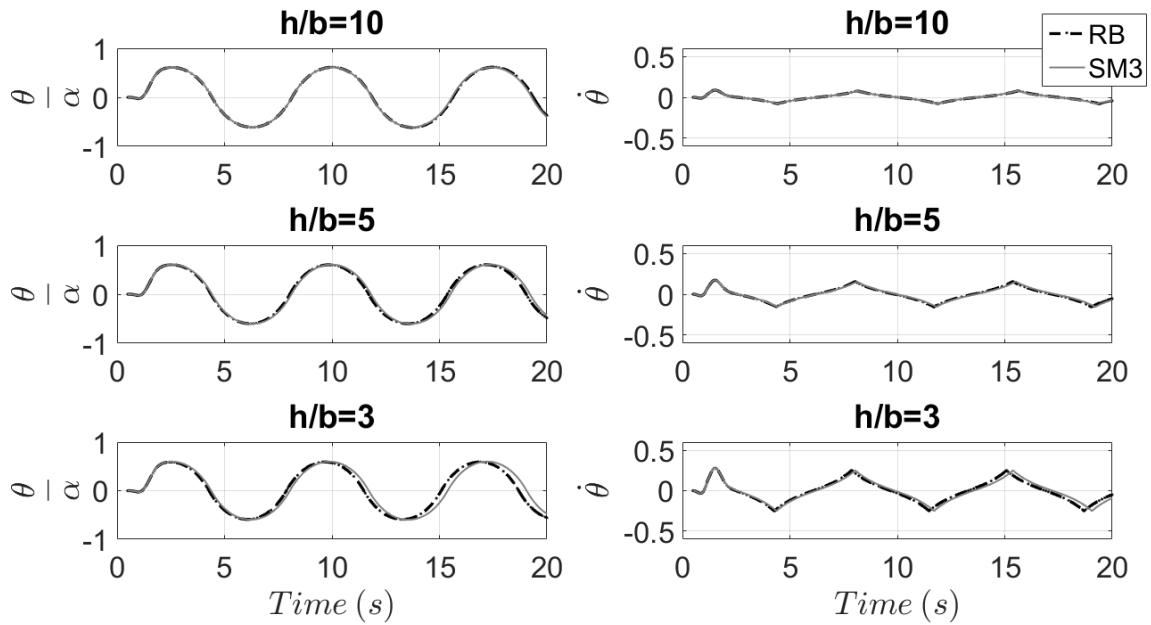


Figure 8: Single degree of freedom Spring Model 3 (SM3).

Figure 9: Comparison of rocking rotation and velocity response history between the rocking block (RB) and the SM3 model for a block with $R = 10m$ subjected to a symmetric Ricker pulse excitation with $\alpha_p = 3.6g \tan \alpha$ and $\omega_p = 1.4\pi$ rad/s.

3.4 Multi-mass Spring Model (mmSM)

We also consider as a fourth model option a multi-mass spring model, denoted as mmSM and shown in Fig. 10. This model is first examined for the rigid block case, but its purpose is for studying the rocking response of flexible bodies where the mass is distributed along the diagonal $2R$ of the block. The model consists of n masses and is identical to a cantilever elastic column with moment of inertia about the pivot point O , equal to $I_o = (1/3)mL^2$, where m is

the total mass and L is the total length. Taking into account the above observation, the moment of inertia of a cantilever with distributed total mass m and length equal to $2R$ about O is: $I_o = (1/3)m(2R)^2 = (4/3)mR^2$ which is equal to the moment of inertia of the rocking block.

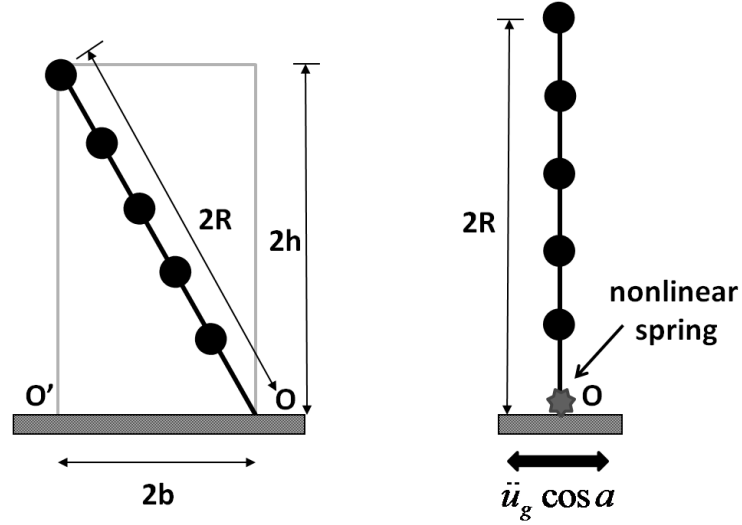


Figure 10: Multi-mass Spring Model (mmSM).

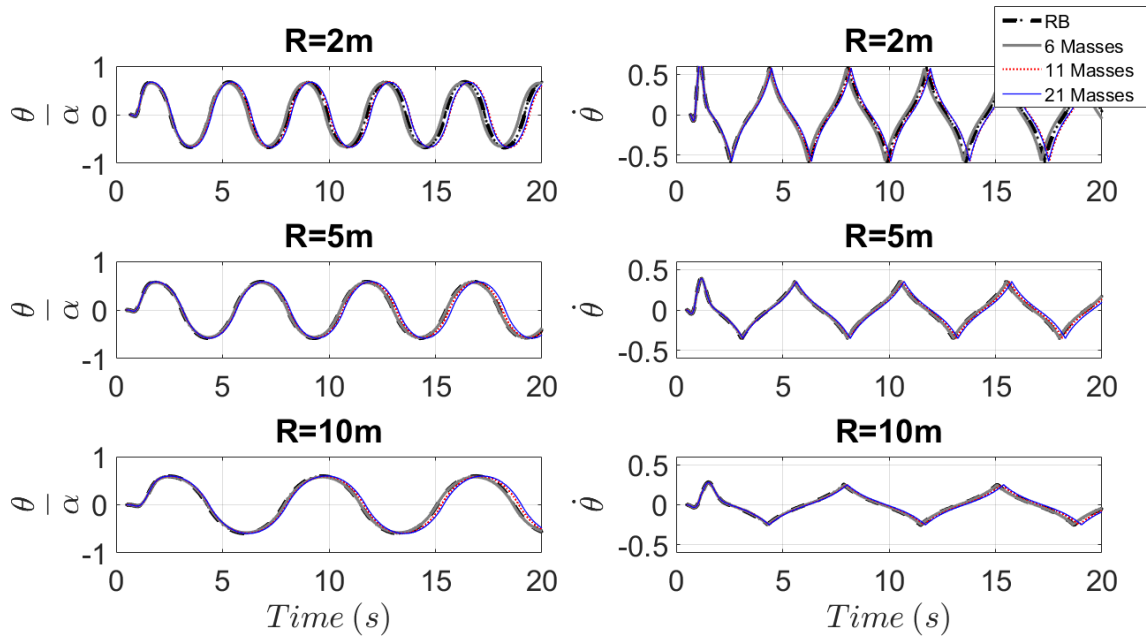


Figure 11: Sensitivity of mmSM for different number of masses considering different blocks with $R = 2, 5, 10m$ and $h/b = 3$ under a symmetric Ricker pulse with $\omega_p = 3\pi, 2\pi, 1.4\pi$ rad/s respectively.

The equations of motion for the mmSM model either taking into account the negative stiffness of the rocking block or considering explicitly second order effects are:

$$I_o \ddot{\theta}(t) + mgR \sin[\alpha \text{sgn} \theta(t) - \theta(t)] = -m(\ddot{u}_g(t) \cos \alpha) R \cos \theta(t) \quad (13)$$

$$I_o \ddot{\theta}(t) + mgR \sin \alpha \operatorname{sgn} \theta(t) [1 - \theta(t) \operatorname{sgn} \theta(t) / \alpha] = -m(\ddot{u}_g(t) \cos \alpha) R \cos \theta(t) \quad (14)$$

$$I_o \ddot{\theta}(t) + mgR [\sin \alpha \operatorname{sgn} \theta(t) - \sin \theta(t)] = -m(\ddot{u}_g(t) \cos \alpha) R \cos \theta(t) \quad (15)$$

Fig. 11 compares the sensitivity to the number of masses for rigid blocks of the same slenderness $h/b = 3$ but different size R . As expected for more stocky blocks and large rotations θ some small error is observed. Moreover, a model with six, or more masses (five and more elements) is sufficient for calculating the seismic response regardless of the block's size.

4 NON-LINEAR STATIC ANALYSIS

The different moment-rotation relationships used for modeling the restoring moments are examined through the pushover curves. When a horizontal force acts at the center of the block, the horizontal force-rotation curve for the rocking block (RB) is:

$$F = \frac{mgR \sin(\alpha - \theta)}{R \cos(\alpha - \theta)} \Rightarrow \frac{F}{mg} = \tan(\alpha - \theta) \quad (16)$$

In the models here proposed, the moment-rotation relationship was introduced taking into account the negative stiffness of the rocking block and is equal to:

$$F = \frac{mgR \sin(\alpha - \theta)}{R \cos \alpha \cos \theta} \Rightarrow \frac{F}{mg} = \frac{\sin(\alpha - \theta)}{\cos \alpha \cos \theta} = \tan \alpha - \tan \theta \quad (17)$$

Note that the above expression does not apply to SM2. Figure 12 compares the pushover curves of Equation 16 and 17 for four slenderness values. Overall, the errors observed are small and increase for small h/b values. A similar comparison when a perfectly-plastic moment rotation

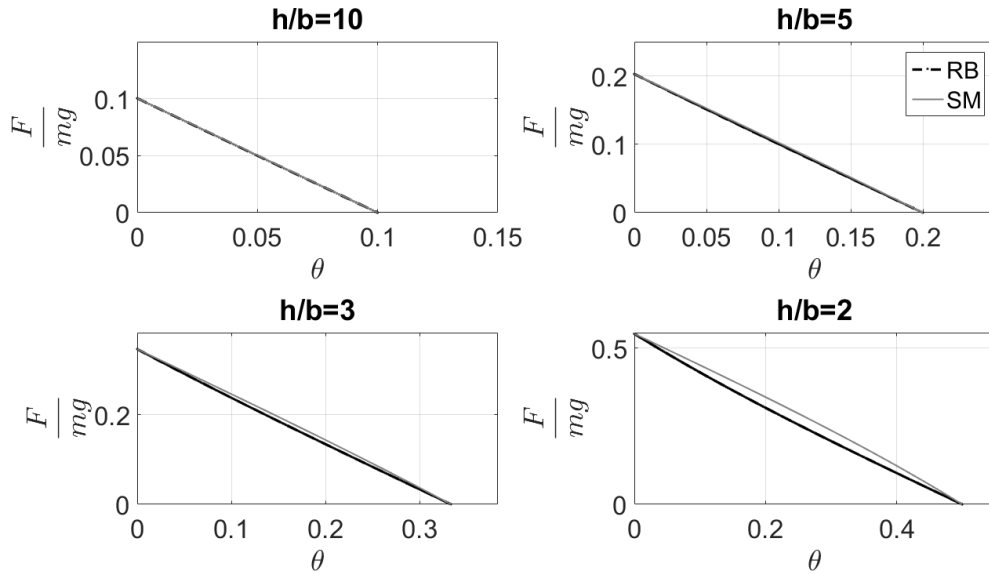


Figure 12: Force-rotation curves for the rocking block (RB) and the spring models (SM).

relationship is combined (Fig. 3c) with second-order effects is shown in Figures 13 and 14. The plots have adopted Equation 18 for SM1 and mmSM and Equation 19 for SM3.

$$F = \frac{mgR(\sin \alpha - \sin \theta)}{R \cos \alpha \cos \theta} \Rightarrow \frac{F}{mg} = \frac{\sin \alpha - \sin \theta}{\cos \alpha \cos \theta} = \frac{\tan \alpha}{\cos \theta} - \frac{\tan \theta}{\cos \alpha} \quad (18)$$

$$F = \frac{mgR(\sin \alpha - \cos \alpha \sin \theta)}{R \cos \alpha \cos \theta} \Rightarrow \frac{F}{mg} = \frac{\sin \alpha - \cos \alpha \sin \theta}{\cos \alpha \cos \theta} = \frac{\tan \alpha}{\cos \theta} - \tan \theta \quad (19)$$

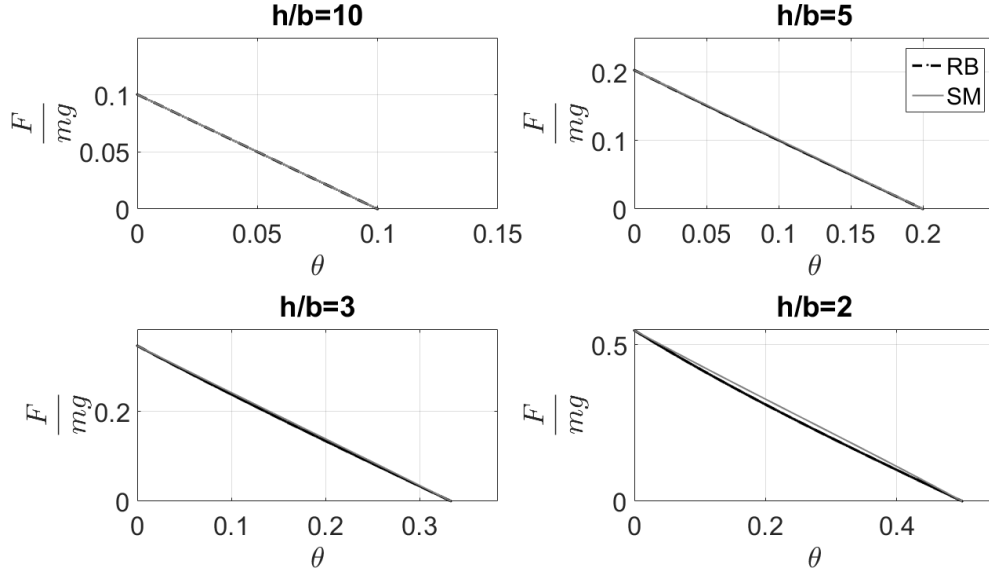


Figure 13: Force-rotation curves for the rocking block (RB) and the SM1 and mmSM.

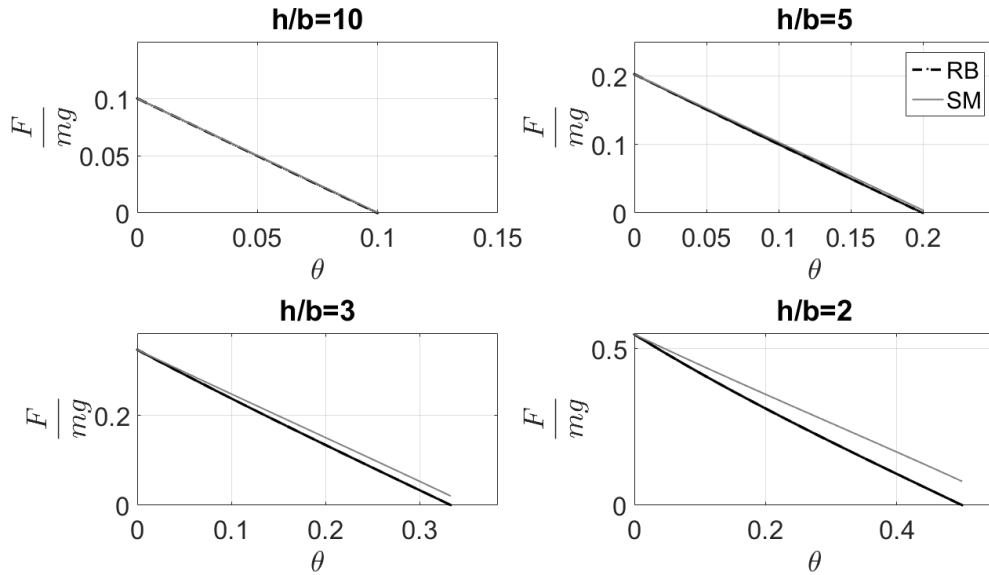


Figure 14: Force-rotation curves for the rocking block (RB) and the SM3.

Figures 13 and 14 show the pushover curves for four different slenderness values. The results are superior for SM1 and mmSM, while for SM3 some small error is observed which becomes more significant for stocky blocks.

It is interesting to also examine overturning moments. The equation of motion of the rocking block and the spring models was obtained from the equilibrium of the restoring and the overturning moment as already discussed. Figure 15 shows the ratio of $M_{ovtn}/(m\ddot{u}_g R)$ and $M'_{ovtn}/(m\ddot{u}_g R)$ for different slenderness values. The models work almost perfectly for slenderness values up to $\tan\alpha = 0.2$ ($h/b = 5$) and small rotations θ .

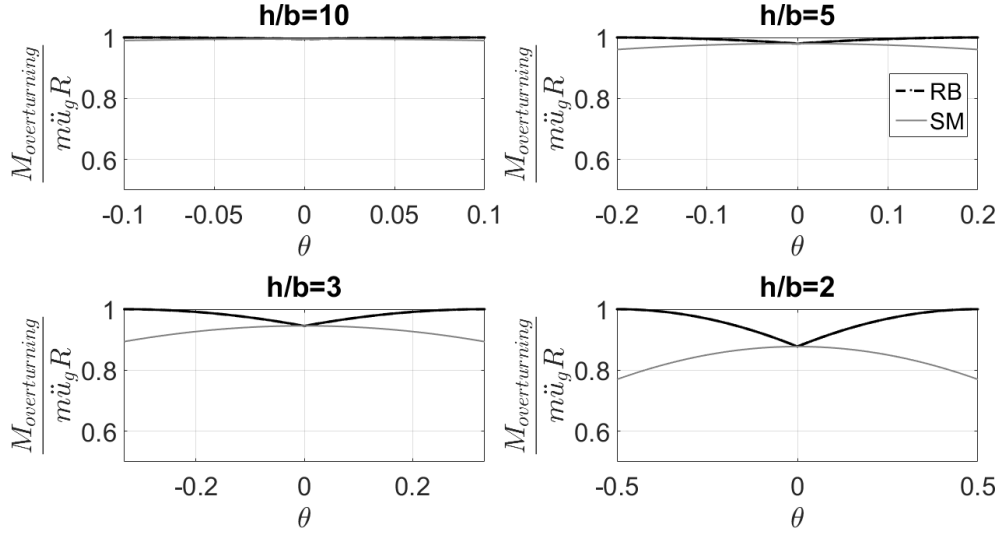


Figure 15: Error of overturning moments predicted by the Spring Models.

5 ROCKING ENERGY DISSIPATION

According to Housner [1], rocking bodies dissipate energy when impact occurs. The instant of the impact the sign of rotation is reversed and the block continues rocking with a new pivot point O' [15]. The principle of conservation of angular momentum just before and right after impact implies:

$$I_o \dot{\theta}_1 - m \dot{\theta}_1 2bR \sin \alpha = I_o \dot{\theta}_2 \quad (20)$$

where $\dot{\theta}_1$ and $\dot{\theta}_2$ is the angular velocity before impact and immediately after it, respectively. Simplifying the above relationship, the coefficient of restitution η is defined as:

$$\eta = \frac{\dot{\theta}_2}{\dot{\theta}_1} = \frac{I_o - 2mR^2 \sin^2 \alpha}{I_o} = \left(1 - \frac{3}{2} \sin^2 \alpha\right) \quad (21)$$

Therefore, the ratio of the kinetic energy before and after impact is estimated by the restitution factor r as:

$$r = \frac{\frac{1}{2} I_o \dot{\theta}_2^2}{\frac{1}{2} I_o \dot{\theta}_1^2} = \left(1 - \frac{3}{2} \sin^2 \alpha\right)^2 = \eta^2 \quad (22)$$

Combining the equation of motion of Eq. 1 with Eq. 21 we can solve the rocking-block problem numerically via a state-space formulation with standard ODE-solvers, as already discussed. This is a form of “event-based” energy dissipation, since energy is dissipated only when an impact (“event”) occurs. Assuming that a body is rocking on a rigid surface, the coefficient of restitution that relates the post-impact with the pre-impact angular velocity can be easily introduced in the proposed models by pausing the analysis when impact is detected. The analysis is then resumed using as “initial” velocity of the subsequent time steps the product of the pre-impact angular velocity of every d.o.f. with the coefficient of restitution. The same procedure is repeated for every impact/event until the analysis is completed.

The results obtained with this practice, match perfectly the results obtained after solving directly the block’s equation of motion as derived by Housner’s theory. Figure 16 shows the

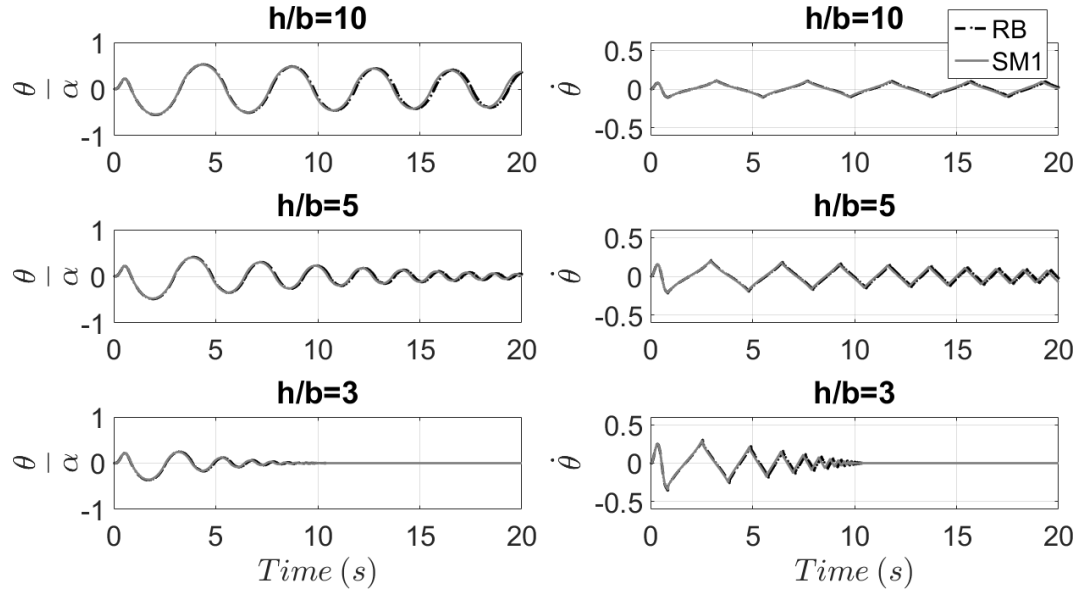


Figure 16: Comparison of rocking rotation and velocity response history between the rocking block (RB) and the event-based damped SM1 model for a block with $R = 5m$ subjected to a sine pulse excitation with $\alpha_p = 3.6g \tan \alpha$ and $\omega_p = 2.66\pi$ rad/s.

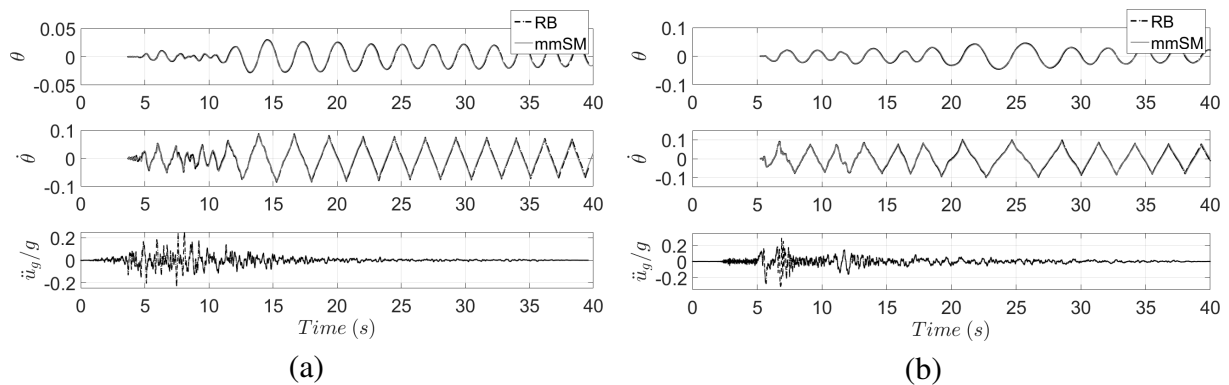


Figure 17: Comparison of rocking rotation and velocity response history between the rocking block (RB) and the event-based damped mmSM model with six-masses for a block with $R = 5m$ and $\tan \alpha = 0.1$ subjected to (a) Loma Prieta's 1989 earthquake (Station: Anderson Dam Downstream, $\phi = 270^\circ$, $PGA = 0.235g$) and (b) Imperial Valleys' 1979 earthquake (Station: Cucapah, $\phi = 85^\circ$, $PGA = 0.309g$).

example of a block for three different h/b values under a pulse-like excitation. Furthermore, Figures 17-19 present examples of blocks with three different R values and two slenderness values subjected to natural records. All analyses confirm that the event-based damping assumption works perfectly and that the proposed FE models can assess the seismic response of a rigid rocking block on a rigid surface.

6 FLEXIBLE BLOCKS

Current research aims to model real structures made of concrete or other materials that are designed to resist seismic loading though rocking. Having studied thoroughly the rocking response of rigid structures, we extend the implementation to the case of flexible blocks. The effect of flexibility is significant when either the ratio $E/\rho g$ is small, or when the size parameter R of the block is large enough. This is better understood from the expression for the first

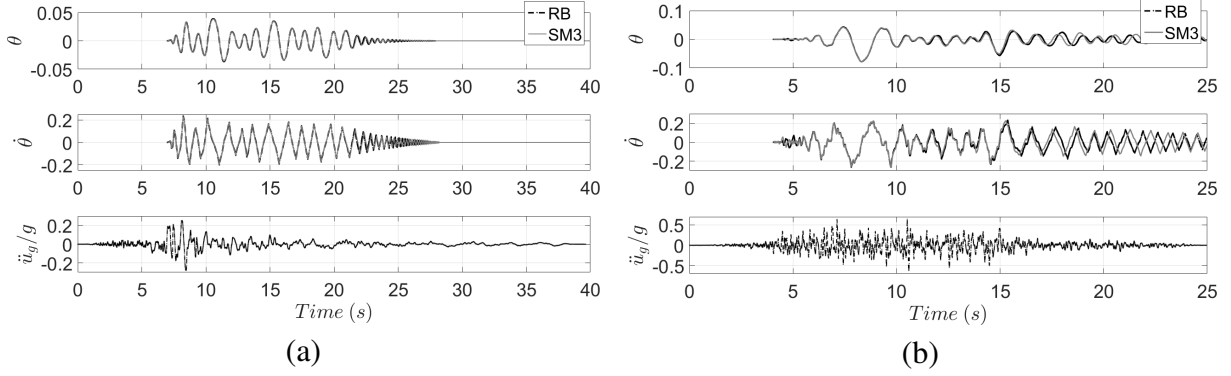


Figure 18: Comparison of rocking rotation and velocity response history between the rocking block (RB) and the event-based damped SM3 model for a block with $R = 2m$ and $\tan \alpha = 1/6$ subjected to Loma Prieta's 1989 earthquake. (a) Station: Hollister Diff Array, $\phi = 255^\circ$, $PGA = 0.279g$ and (b) Station: Waho, $\phi = 90^\circ$, $PGA = 0.638g$.

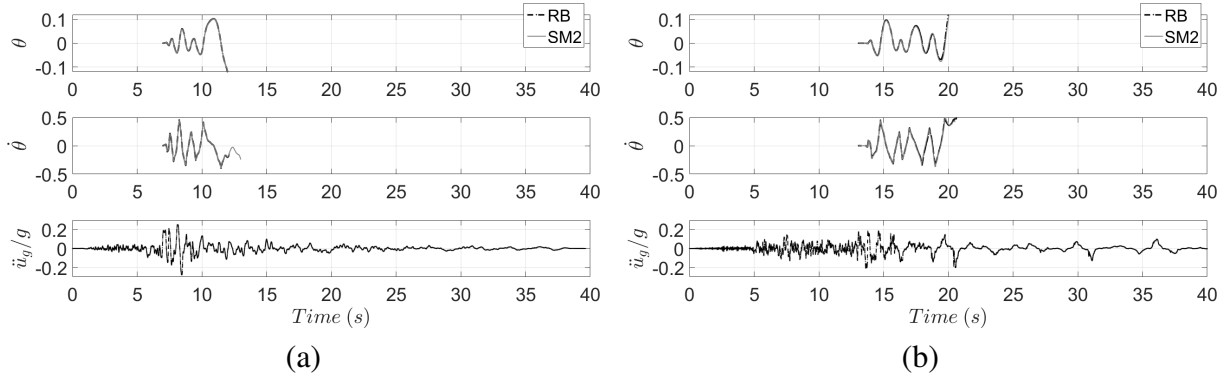


Figure 19: Comparison of rocking rotation and velocity response history between the rocking block (RB) and the event-based damped SM2 model for a block with $R = 1m$ and $\tan \alpha = 1/6$ subjected to (a) Loma Prieta's 1989 earthquake (Station: Hollister Diff Array, $\phi = 255^\circ$, $PGA = 0.279g$) and (b) Superstition Hills' 1987 earthquake (Station: Wildlife Liquefaction Array, $\phi = 360^\circ$, $PGA = 0.20g$).

eigenperiod of flexible homogeneous rectangular blocks [4]:

$$T_1 = 12.38 \sqrt{\frac{\rho}{E} \frac{h}{\tan \alpha}} \quad (23)$$

Flexibility increases the overturning acceleration due to the transformation of the rotational kinetic energy to bending vibrations at each rocking impact. Below we study the mmSM model for the modeling of flexible rocking blocks (FRB). For the case studies considered, the are made of concrete and have $E = 30GPa$ and $\rho = 2.5Mg/m^3$.

Figure 20 shows the response when the block is subjected to a sine pulse, while Figure 21 shows the response when a natural record is imposed (no damping). The flexible block was also modeled with a full mesh of quadrilateral elements in Abaqus [16]. The estimate of the top displacement of the column $u_{top} = u \cos \alpha$ is compared in Figures 20a and 21a. Figures 20b and 21b plot the top displacement of the column due to bending, $w_{top} = u_{top} - 2R \cos \alpha \sin \theta$, obtained as the difference between the total top displacement and the top displacement due to base rotation (similar to that of a rigid body). We observe that the effect of column flexibility is not significant for solitary blocks up to 30m tall, as already discussed in reference [4]. To confirm this, a rigid and a flexible block are compared in Figures 22 and 23 for different R and α values.

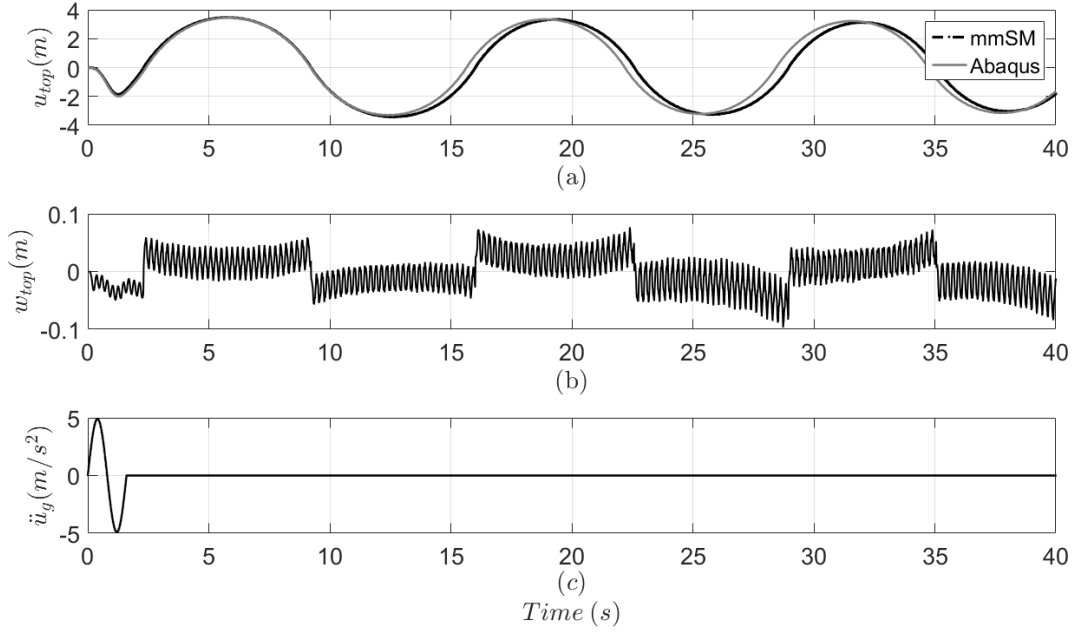


Figure 20: (a) Comparison of top displacement time history response between a flexible rocking block with $2h = 50m$ and $\tan \alpha = 0.1$ modeled in Abaqus and the proposed mmSM with six masses, (b) top displacement due to bending, and (c) the sine pulse excitation with $T_p = 1.6sec$ and $a_p = 5g \tan \alpha = 4.905m/sec^2$.

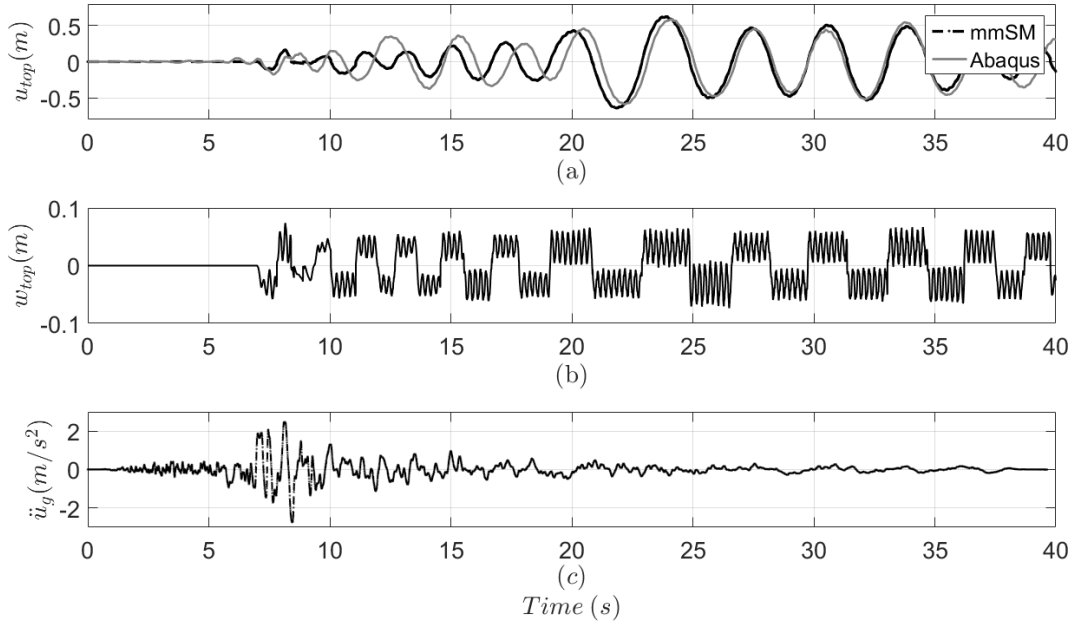


Figure 21: (a) Comparison of top displacement time history response between a flexible rocking block with $2h = 50m$ and $\tan \alpha = 0.1$ modeled in Abaqus and the proposed mmSM with six masses, (b) top displacement due to bending, and (c) the Loma Prieta's 1989 earthquake (Station: Hollister Diff Array, $\phi = 255^\circ$, $PGA = 0.279g$).

In Figures 22 and 23 we show the results of event-based damping using the coefficient of restitution obtained from Equation 21. Furthermore, Rayleigh damping is also applied on the flexible column using a damping ratio of $\zeta = 0.01$. We have chosen to apply only some minor damping since most of the energy dissipation is due to rocking. The first row of Figure 22

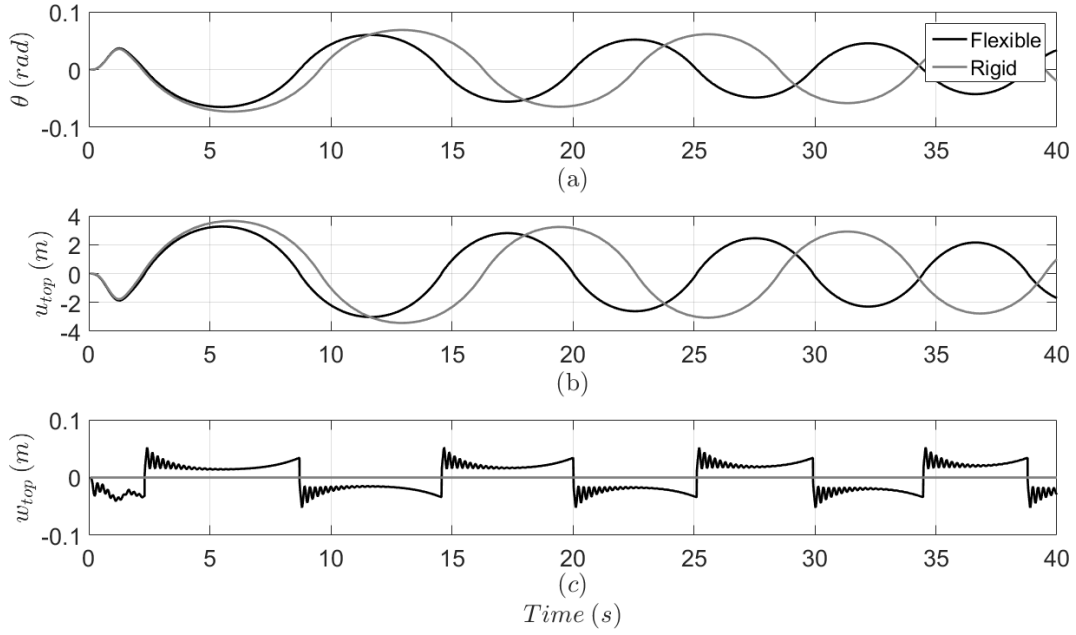


Figure 22: Comparison of (a) rotation, (b) top displacement and (c) top displacement due to bending time history response between a flexible and a rigid block with $2h = 50m$ and $\tan \alpha = 0.1$ subjected to a sine pulse excitation with $T_p = 1.6sec$ and $a_p = 5g \tan \alpha = 4.905m/sec^2$.

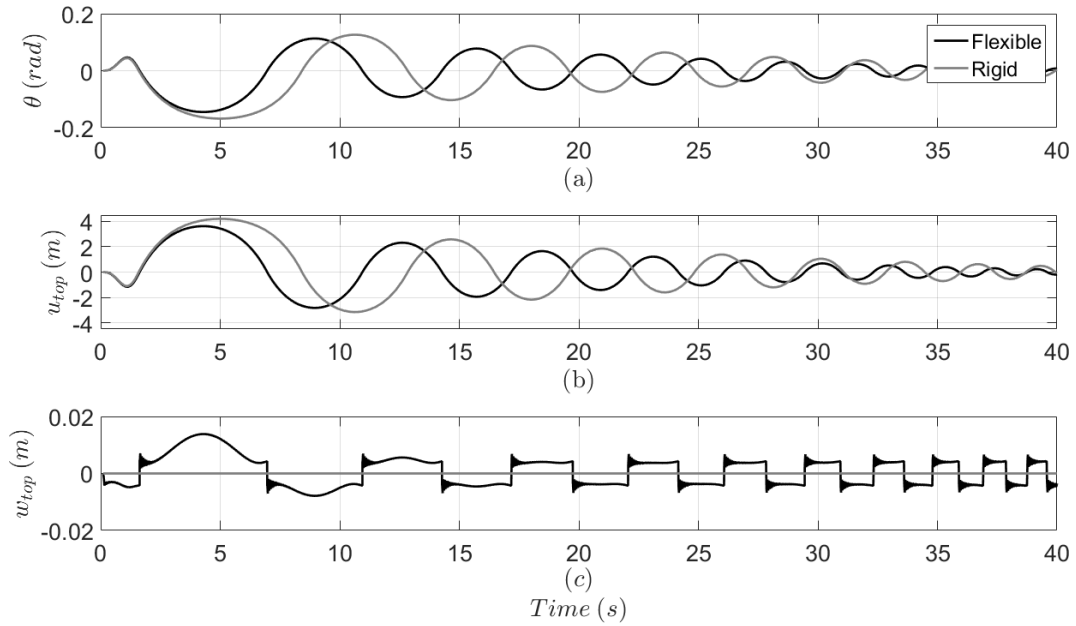


Figure 23: Comparison of (a) rotation, (b) top displacement and (c) top displacement due to bending time history response between a flexible and a rigid block with $2h = 25m$ and $\tan \alpha = 0.2$ subjected to a sine pulse excitation with $T_p = 1.6sec$ and $a_p = 2.7g \tan \alpha = 5.297m/sec^2$.

and 23 plot the rotation at the base of the column, the second row show the top displacement and the third row the top displacement due to bending. Top displacement due to bending is indeed negligible compared to the total displacement of the top (Fig. 23c) and for a block with $2h = 25m$. However, this may differ if a different seismic record is considered.

7 CONCLUSIONS

Different simple spring models for the analysis of rigid or flexible rocking bodies are considered. The models are first verified against the numerical solution of Housner's theory for a solitary rigid rocking block and the results were excellent. The response of flexible blocks were then examined and verified against the results of Abaqus. The seismic response assessment of rigid and flexible blocks led to the conclusions below:

- The rocking problem can be solved with single-degree-of-freedom finite element models based on beam-column elements connected to a zero-length elastic rotational spring.
- We have examined three different moment-rotation relationships and we studied their performance on different FE models.
- The primary source of error between the rocking block and the models is in the term of the overturning moment. The errors are acceptable and the models produce results almost identical to those of solving directly the block's equation of motion.
- A second goal is the assessment of the seismic response of flexible rocking blocks. A six-mass spring model was tested against the response obtained if the block was modeled with a full mesh of quadrilateral elements in Abaqus. The proposed model produced accurate results within a fraction of the required CPU time.
- "Event-based" damping is proposed as the safest and most accurate way to model energy dissipation for both rigid and flexible rocking systems.

8 ACKNOWLEDGEMENTS

The financial support provided by the European Research Council Advanced Grant "MASTER Mastering the computational challenges in numerical modelling and optimum design of CNT reinforced composites" (ERC-2011-ADG 20110209) is gratefully acknowledged.

REFERENCES

- [1] G.W. Housner, The behavior of inverted pendulum structures during earthquakes. *Bulletin of the Seismological Society of America*, **53**(2), 404–417, 1963.
- [2] N. Makris, D. Konstantinidis, The rocking spectrum and the limitations of practical design methodologies. *Earthquake Engineering and Structural Dynamics*, **32**, 265–289, 2003.
- [3] J. Milne, Seismic Experiments. *Transactions of the Seismological Society of Japan*, **8**, 1–82, 1885.
- [4] M.F. Vassiliou, K.R. Mackie, B. Stojadinović, Dynamic response analysis of solitary flexible rocking bodies: modeling and behavior under pulse-like ground excitation. *Earthquake Engineering and Structural Dynamics*, **46**(3), 447–466, 2016.
- [5] M.F. Vassiliou, K.R. Mackie, B. Stojadinović, A finite element model for seismic response analysis of deformable rocking frames. *Earthquake Engineering and Structural Dynamics*, **43**(10), 1463–1481, 2014.

- [6] I.N. Psycharis, Dynamics of flexible systems with partial lift-off. *Earthquake Engineering and Structural Dynamics*, **11**(4), 501–521, 1983.
- [7] M. Apostolou, G. Gazetas, E. Garini, Seismic response of slender rigid structures with foundation uplifting. *Soil Dynamics and Earthquake Engineering*, **27**(7), 642–654, 2007.
- [8] S. Acikgoz, M.J. DeJong, The interaction of elasticity and rocking in flexible structures allowed to uplift. *Earthquake Engineering and Structural Dynamics*, **41**(15), 2177–2194, 2012.
- [9] A.K. Chopra, F. McKenna, Modeling viscous damping in nonlinear response history analysis of buildings for earthquake excitation. *Earthquake Engineering and Structural Dynamics*, **45**(2), 193–211, 2016.
- [10] C.S. Yim A. K. Chopra, J. Penzien, Rocking Response of Rigid Blocks to Earthquakes. *Earthquake Engineering and Structural Dynamics*, **8**, 565–587, 1980.
- [11] M.J. DeJong, E.G. Dimitrakopoulos, Dynamically equivalent rocking structures. *Earthquake Engineering and Structural Dynamics*, **43**, 1543–1563, 2014.
- [12] E.G. Dimitrakopoulos, M.J. DeJong, Revisiting the rocking block: closed-form solutions and similarity laws. *Proceedings of the Royal Society of London A: Mathematical, Physical and Engineering Sciences*, 468, 2012.
- [13] Matlab Version 2015b. The Language of Technical Computing.
- [14] OpenSEES (Open System for Earthquake Engineering Simulations). opensees.berkeley.edu
- [15] J. Zhang, N. Makris, Rocking response of free-standing blocks under cycloidal pulses. *Journal of Engineering Mechanics, ASCE*, **127**(5), 473–483, 2001.
- [16] Abaqus, Version 6.14, SIMULIA (ABAQUS Inc., Providence, USA).